Photosynthesis Research (2022) 151:235–250
https://doi.org/10.1007/s11120-021-00877-5

ORIGINAL ARTICLE

Cyclic electron flow (CEF) and ascorbate pathway activity provide constitutive photoprotection for the photopsychrophile, *Chlamydomonas* sp. UWO 241 (renamed *Chlamydomonas priscuii*)

Sarah Stahl-Rommel[1,2] · Isha Kalra[1] · Susanna D'Silva[1] · Mark M. Hahn[1] · Devon Popson[1] · Marina Cvetkovska[3] · Rachael M. Morgan-Kiss[1,4]

Received: 27 May 2021 / Accepted: 13 September 2021 / Published online: 5 October 2021

Abstract

Under environmental stress, plants and algae employ a variety of strategies to protect the photosynthetic apparatus and maintain photostasis. To date, most studies on stress acclimation have focused on model organisms which possess limited to no tolerance to stressful extremes. We studied the ability of the Antarctic alga *Chlamydomonas* sp. UWO 241 (UWO 241) to acclimate to low temperature, high salinity or high light. UWO 241 maintained robust growth and photosynthetic activity at levels of temperature (2 °C) and salinity (700 mM NaCl) which were nonpermissive for a mesophilic sister species, *Chlamydomonas raudensis* SAG 49.72 (SAG 49.72). Acclimation in the mesophile involved classic mechanisms, including downregulation of light harvesting and shifts in excitation energy between photosystem I and II. In contrast, UWO 241 exhibited high rates of PSI-driven cyclic electron flow (CEF) and a larger capacity for nonphotochemical quenching (NPQ). Furthermore, UWO 241 exhibited constitutively high activity of two key ascorbate cycle enzymes, ascorbate peroxidase and glutathione reductase and maintained a large ascorbate pool. These results matched the ability of the psychrophile to maintain low ROS under short-term photoinhibition conditions. We conclude that tight control over photostasis and ROS levels are essential for photosynthetic life to flourish in a native habitat of permanent photooxidative stress. We propose to rename this organism *Chlamydomonas priscuii.*

Keywords Antarctica · Ascorbate · Cyclic electron flow · Photosystem I · Psychrophile · ROS

Abbreviations

A_{820}	Absorbance at 820 nm
ΦPSII	Yield of photosystem II
APX	Ascorbate peroxidase
AsA-GSH	Ascorbate–glutathione pathway
C	Control
CAT	Catalase
CBB	Calvin Benson Bassham
CEF	Cyclic electron flow
FR	Far red
F_V/F_M	Maximum photosynthetic efficiency of photosystem II
GR	Glutathione reductase
H_2DCFDA	2′,7′-Dichlorodihydrofluorescein diacetate
HL	High light
HS	High salt
LHCI	Light harvesting complex I
LHCII	Light harvesting complex II
LHCSR	Light harvesting complex stress related protein
LT	Low temperature
qL	Photochemical quenching
MDHAR	Dehydroascorbate reductase
NBT	Nitroblue tetrazolium
NPQ	Nonphotochemical quenching
PGR5	Proton gradient regulation 5 protein
PGRL1	PGR5-like protein 1
pmf	Proton motive force
PQ	Plastoquinone

✉ Rachael M. Morgan-Kiss
morganr2@miamioh.edu

[1] Department of Microbiology, Miami University, Oxford, OH 45045, USA

[2] Present Address: JES Tech, Houston, TX 77058, USA

[3] Department of Biology, University of Ottawa, Ottawa, ON K1N 6N5, Canada

[4] Department of Microbiology, Miami University, 700 E High St., 212 Pearson Hall, Oxford, OH 45056, USA

PSI	Photosystem I
PSII	Photosystem II
ROS	Reactive oxygen species
RT-qPCR	Real time quantitative PCR
SOD	Super oxide dismutase
$t_{½}^{red}$	Half-time for P700 re-reduction

Introduction

Photostasis is a phenomenon common to all photosynthetic organisms: it encompasses processes which contribute to cellular homeostasis by balancing rates of photosynthetic energy absorbed with energy consumed by metabolism (Öquist and Hüner 2003). Disruption of photostasis is manifested as an accumulation of a reduced pool of the mobile electron acceptor, plastoquinone (PQ), leading to photooxidative stress. This phenomenon occurs under excessive light conditions; however, any environmental condition which impacts an organism's ability to use absorbed light energy can lead to an over-reduction of the PQ pool (Hüner et al. 2012; Morgan-Kiss et al. 2006). Thus, any alteration in an organism's environment can exacerbate disruption to photostasis and enhance the probability of photooxidative stress, including day/night cycle, salinity, drought, heat, chilling, and nutrient status (Bartels and Sunkar 2005; Ensminger et al. 2006; Sharma et al. 2012; Takahashi and Murata 2008; Liu et al. 2012).

A major biproduct of unbalanced photosynthesis is the production of reactive oxygen species (ROS). ROS accumulates when the photosynthetic electron transport chain becomes over-reduced, causing oxidative injury and damage to proteins, lipids, nucleic acids, and many components of the photosynthetic apparatus (Asada 1996; Apel and Hirt 2004; Møller et al. 2007; Sirikhachornkit and Niyogi 2010). Oxidative stress responses are influenced by time scale and can be classified into mechanisms for short-term, acute oxidative stress occurring over seconds to minutes, or long-term, constitutive stress occurring over hours to years (Niyogi 1999; Suzuki et al. 2012). Short-term responses are non-heritable adjustments to physiology and biochemistry which avoid ROS production (Sirikhachornkit and Niyogi 2010; Ledford et al. 2007). Common short-term stress response mechanisms are phototaxis, state transitions, nonphotochemical quenching (NPQ), and alternative electron transport pathways, such as the water-water cycle and PSI-associated CEF (Asada 2000; Cournac et al. 2002; Minagawa 2011; Müller et al. 2001; Witman 1993). In *C. reinhardtii*, induction of NPQ requires the Light Harvesting Complex Stress Related proteins (LHCSRs), LHCSR1 and LHCSR3 (Maruyama et al. 2014; Peers et al. 2009).

Changes in gene expression and protein translation aid in maintenance of photostasis over longer time scales. Long-term responses can involve minimizing ROS production and/or increasing ROS detoxification, including changes to antenna size or PSI/PSII stoichiometry increased CO_2 fixation capacity, and activation of antioxidant pathways (Asada 2006; Falk et al. 1993; 1994; Tanaka and Melis 1997; Lucker and Kramer 2013; Yamori et al. 2016). Enzymatic antioxidants used for ROS detoxification include superoxide dismutase (SOD), catalase (CAT), and enzymes of the ascorbate–glutathione (AsA-GSH) cycle (Noctor and Foyer 1998). Maintenance of high antioxidant capacity has been associated with tolerance to environmental stress in plants and algae (Aldesuquy et al. 2013; Chen et al. 2011; Van Alstyne et al. 2020). The AsA-GSH pathway is particularly important for antioxidative defense in plants but appears to play a lesser role in algae and cyanobacteria (Foyer and Halliwell 1976; Foyer et al. 1997; Hu et al. 2008).

Some photosynthetic organisms have evolved to survive and grow in permanent stressful environments. Relative to the well-studied processes of short- and long-term stress acclimation, strategies of photosynthetic adaptation to permanent abiotic stress are significantly less understood. Low temperature environments are abundant at high latitudes (Young and Schmidt 2020): photopsychrophiles are photosynthetic organisms which are physiologically adapted to permanent low temperatures (Morgan-Kiss et al. 2006). The Antarctic *Chlamydomonas* sp. UWO 241 (UWO 241) resides in the deep photic zone of a permanently ice-covered, hypersaline lake (Lake Bonney, McMurdo Dry Valleys, Antarctica). UWO 241 is one of the few models for photosynthetic adaptation to combined low temperatures and high salinity (Cvetkovska et al. 2017). Early studies reported that UWO 241 exhibits minimal capacity for short-term acclimatory mechanisms, such as the xanthophyll cycle and state transitions (Morgan et al. 1998; 2002b), and sensitivity to short-term thermal or high light stress (Morgan-Kiss et al. 2002a; Pocock et al. 2007). In lieu of short-term acclimation, UWO 241 has evolved to rely on constitutive mechanisms as a consequence of adaptation to permanent low temperatures and high salinity (Morgan-Kiss et al. 2006). While UWO 241 exhibits high susceptibility to high light stress, it also possesses the ability to rapidly recover from photoinhibition (Pocock et al. 2007). Despite the presence of cold-active thylakoid kinases, it lacks state transitions and energy transfer from PSII to PSI may occur though a poorly understood spill-over mechanism (Szyszka-Mroz et al. 2019).

Under native low temperature and high salinity conditions, UWO 241 forms a novel PSI supercomplex which allows the organism to maintain a strong capacity for PSI-driven CEF (Cook et al. 2019; Szyszka-Mroz et al. 2015). The additional proton motive force (pmf) derived from CEF is used for constitutive capacity for NPQ and production of additional ATP in cells grown under high salinity (Kalra et al. 2020). The adjustments to the photosynthetic

apparatus are accompanied by alterations in carbon metabolism, including upregulation of several enzymes within the Calvin Benson Bassham cycle (CBB), and key enzymes of the shikimate pathway, a high carbon flux pathway which synthesizes precursors for aromatic metabolites (Kalra et al. 2020; Julkowska 2020). Together, these novel adaptive strategies allow UWO 241 to maintain robust growth and photosynthesis under the combined stress of permanent low temperature and high salinity.

Acclimation is the capacity of an organism to the return to cellular homeostasis following an initial disruption in cellular processes due to the action of environmental stressors (Borowitzka 2018). While activation of CEF is known to be essential in plants and algae exposed to short-term stress, the discovery of a strong CEF capacity in a psychrophilic, halotolerant alga suggests that there is an unappreciated role for CEF during acclimation to persistent environmental stress. We hypothesized that UWO 241 utilizes CEF and ROS detoxification as long-term stress acclimation mechanisms to maintain photostasis and protect the photosynthetic apparatus from photooxidative damage. We tested this hypothesis by comparing growth physiology as well as PSII and PSI photochemistry in UWO 241 and a related mesophilic species, *Chlamydomonas raudensis* SAG 49.72, during acclimation to high light, low temperature and high salinity. We also monitored production of a major ROS (O_2^-) as well as activity of two key enzymes of the AsA-GSH pathway (Ascorbate Peroxidase, APX; Glutathione Reductase, GR). Our study shows that UWO 241 possesses robust ability for long-term acclimation by both avoiding ROS production and relying on constitutive ROS detoxification. We suggest that tight control over ROS production/destruction allows this extremophile to survive and thrive under long-term exposure to multiple environmental stressors in its native habitat.

Materials and methods

Strains, growth conditions and growth physiology

Cultures of the psychrophilic *Chlamydomonas* sp. UWO 241 (CCMP1619) and a mesophilic strain, *Chlamydomonas raudensis* SAG 49.72, were grown in Bold's basal medium (BBM) (Nichols and Bold 1965) under ambient CO_2 conditions in 250 mL Pyrex tubes submerged in temperature-regulated aquaria as described in Morgan-Kiss et al. (2008). The mesophilic SAG 49.72 was chosen for comparison as it has been used in several comparative studies with UWO 241 (Pocock et al. 2011; Szyszka et al. 2007; Szyszka-Mroz et al. 2015, 2019). Cultures were grown under either control (C) conditions or exposed to one of three long-term stress treatments: high light (HL), low temperature (LT) or high salt (HS). For control conditions, cultures were grown under temperature/light regimes of 8 °C/50 µmol $^{-2}$ s^{-1} and 20 °C/50 µmol $^{-2}$ s^{-1} for UWO 241 and SAG 49.72, respectively, and NaCl levels of 0.43 mM for both strains (Table 1). Conditions were chosen based on previous studies (Pocock et al. 2011; Szyszka et al. 2007; Morgan-Kiss et al. 2006) to reflect the maximum level of a particular stress to which the organism could fully acclimate and not show chronic stress symptoms, that is achieve exponential growth and high photochemical activity (maximum photosynthetic efficiency values, F_V/F_M, above 0.5). Long-term stress conditions for UWO 241 and SAG 49.72, respectively, were: (i) high light, 250 µmol m^{-2} s^{-1} and 500 µmol m^{-2} s^{-1}; (ii) low temperature, 2 °C and 11 °C; (iii) high salinity, 700 mM NaCl and 100 mM NaCl.

Growth kinetics were monitored as change in optical density at 750 nm. All other measurements were performed on mid-log phase cultures. Chlorophyll a and b concentrations were determined from whole cell extractions in 90% acetone according to Jeffry and Humphrey (1975).

Room temperature chlorophyll fluorescence

The activities of PSI and PSII were measured in dark-adapted (10 min) exponentially growing cultures with a Dual-PAM-100 system (Heinz Walz GmbH, Effeltrich, Germany) as described in Szyska et al. (2007). All samples were supplemented with 10 mM sodium bicarbonate and measurements were performed in a water-jacketed cuvette at the corresponding growth temperatures. The fluorescence parameters F_V/F_M (maximum photochemical efficiency), qL (proportion of open PSII reaction centers, assuming the "lake" model for antenna connectivity between reaction centers, qL = qP· [Fo′/FS]), Φ (PSII) (quantum yield of photochemistry, ΦPSII = (Fm ′ − Fs) /Fm′,), and NPQ (nonphotochemical energy dissipation from antenna

Table 1 Growth conditions for UWO 241 and SAG 49.72 used in this study

Growth condition	UWO 241	SAG 49.72
Control (C)	8 °C/0.43 mM NaCl/50 µmol m^{-2} s^{-1}	20 °C/0.43 mM NaCl/50 µmol m^{-2} s^{-1}
High light (HL)	250 µmol m^{-2} s^{-1}	500 µmol m^{-2} s^{-1}
Low temperature (LT)	2 °C	11 °C
High salinity (HS)	700 mM NaCl	100 mM NaCl

quenching—Fm – Fm ′)/Fm′, were calculated during steady state photosynthesis (Kramer et al. 2004). All measurements were performed under temperature and irradiance values which matched the growth conditions.

Low temperature Chl a fluorescence (77 K)

Low temperature (77 K) Chl fluorescence emission spectra were measured using a Perkin Elmer Luminescence Spectrometer (LS50B) (Buckinghamshire, England) equipped with liquid nitrogen accessory. Algal cultures (~ 250 µL) from dark-adapted (10 min) mid-log phase cultures were transferred to NMR tubes and flash frozen in liquid nitrogen. Fluorescence spectra were collected at the excitation wavelength of 435 nm and recorded at a slit width of 4 nm for excitation and emission. Decompositional analysis of fluorescence emission spectra in terms of five Gaussian bands was performed by a non-linear least squares algorithm according to Morgan-Kiss et al. (2002a) using the program OriginPro 8.5.1.

P700 reduction/oxidation kinetics

Far red induced photooxidation of P700 was used to determine rates of CEF as described by Morgan-Kiss et al. (2002b). A volume of exponential phase cultures representing 25 µg Chl a was dark-adapted for 10 min and then filtered onto 25 mm GF/C filters (Whatman, Cat No. 1822–025). Filters were measured on the Dual-PAM 100 instrument using the leaf attachment. The proportion of photooxidizable P700 was determined by monitoring absorbance changes at 820 nm and expressed as the parameter ($\Delta A_{820}/A_{820}$). The signal was balanced, and the measuring light switched on. Far red (FR) light (λmax = 715 nm, 10 Wm^{-2}, Scott filter RG 715) was then switched on to oxidize P700. The half time for the reduction of $P700^+$ to P700 ($t_{½}^{red}$) was calculated as an estimate of relative rates of PSI-driven CEF (Ivanov et al. 1998; Kalra et al. 2020). The re-reduction time for P700 was calculated using the program OriginPro 8.5.1 using first order exponential decay kinetics.

ROS

Superoxide (O_2^-) and H_2O_2 levels were semi-quantified according Förster et al. (2005) with some modifications. A volume representing ~ 12,500 cells of UWO 241 or SAG 49.72 mid-log phase cultures grown under control conditions was treated with 20 µL of 1 mM nitroblue tetrazolium (NBT; Sigma) or 5 mM 3,3'-diaminobenzidine-HCL (DAB; Sigma) for O_2^- or H_2O_2 detection, respectively, in the dark for 5 min prior to the stress treatment. Samples were then filtered onto 25 mm GF/C filters (Whatman, Cat No. 1822–025) and exposed to short-term stress either LT (5 °C) or HL (300 µmol m^{-2} s^{-1}) in an AlgaeTron 130 growth incubator (Photon Systems Instruments, Czech Republic) for up to 1 h. Following treatment, filters were immediately immersed in 80% acetone to remove Chl, and then allowed to dry in a fume hood prior to imaging. O_2^- levels were measured semi-quantitatively by densitometric analyses using the program ImageJ (http://imagej.nih.gov/ij/). H_2O_2 was also quantified using the fluorescent dye H_2DCFDA (Invitrogen) as described by the methods in Pérez-Pérez et al. (2012) with some modifications. Cells were pelleted by centrifugation and resuspended in 10 mM TRIS–HCl pH = 7.3. Cells were then broken by bead beating (2 × 30 s cycles) and stored at -80˚C until use. Samples (90 µg total protein) were incubated for 30 min at 30 °C, and transferred to a 96-well plate and fluorescence was measured using a plate reader (SpectraMax iD5, Molecular Devices), with an excitation and emission wavelengths of 485 nm and 535 nm respectively.

Ascorbate Pathway

Glutathione reductase (GR) activity was measured using a glutathione reductase assay kit based on NADPH oxidations (Kit 703,202, Cayman Chemicals, Ann Arbor). Mid-log phase cultures (~ 3–10 × 10^6 cells) were collected by centrifugation and resuspended in GR assay buffer (50 mM potassium phosphate, 1 mM EDTA, pH 7.5). Cells were lysed by 4 × 30 s beadbeating cycles. Twenty microliters of lysed cell supernatant was mixed with 100 µL GR assay buffer and 20 µL oxidized glutathione. The reactions were initiated with 50 µL NADPH, and oxidation of NADPH was measured kinetically over 10 min at 340 nm at an assay temperature of 25 °C. Activity was calculated by ΔA_{340} min^{-1} mg^{-1} protein using an NADPH extinction coefficient of 0.00373 μM^{-1}.

APX activity was measured according to Venisse et al. (2001) with some modifications. Sample extracts were prepared as described for the GR activity assay. Ten microliters of supernatant was added to 190 µL of reaction buffer (50 mM potassium phosphate buffer, pH 7.8), supplemented with 0.5 mM ascorbic acid and 0.1 mM hydrogen peroxide. Oxidation of ascorbate was monitored spectrophotometrically as a decrease A_{290} (extinction coefficient 0.00168 μM^{-1}) over 10 min to determine APX activity (Venisse et al. 2001).

For ascorbate quantitation, the protocol of Kovács et al. (2016) was followed with some modifications. 25 mL of culture (6 to 7 × 10^7 total cells) was pelleted and washed once in HPLC grade H_2O. Pellets were resuspended in an extracted in 2 mM ETA containing 5 mM dithiothreitol and 1% orthophosphoric acid. Cells were broken using a bead beater (2 × 30 s cycles) and samples were centrifuged for 30 min at 19,000 × g and total cellular ascorbate levels (ascorbate + dehydroascorbate) were determined using a

commercial kit (Ascorbate Assay Kit, Cayman Chemical. #700,420).

The genome and transcriptome of UWO 241 were sequenced and assembled as described before (Cvetkovska et al. 2019; Raymond & Morgan-Kiss 2013; Zhang et al. 2021). The assembled genome and transcriptome dataset are deposited at NCBI database under BioProject accessions PRJNA547753 and PRJNA575885, respectively. These datasets were screened for the presence of the genes encoding for enzymes of the AsA-GSH cycle. Previously identified genes from the model alga *Chlamydomonas reinhardtii* were obtained from the Phytozome database (v12, Joint Genome Institute) and used as a query. Genomic sequences with a high degree of identity (E-value cutoff 10^{-20}) were obtained and annotated using Geneious Prime (Biomatters Ltd, Auckland, New Zealand).

The amino acid sequence was predicted based on the gene coding sequence, and the identity of the enzyme was confirmed based on conserved motifs (Pitsch et al. 2010; Wu and Wang 2019). Multiple sequence alignments were performed using Clustal Omega (Sievers and Higgins 2018), and protein localization was predicted using PSORT (Horton et al. 2007) and PredAlgo (Tardif et al. 2012). Sequence data for the UWO 241 genes can be found in GenBank/EMBL database under accession numbers listed in Tables S1 and S2.

RNA isolation and RT-qPCR

Total RNA was isolated from UWO241 cultures grown under control and long-term stress conditions in mid-log phase using the Maxwell 16 LEV Plant RNA Kit (Promega, Cat No. AS1430). RNA extraction was performed according manufacturer's instructions with a few minor changes. Cell pellets from 25 mL of culture were resuspended in 700 µL Homogenization buffer, transferred to a Lysing Matrix E tube (MP Biomedicals, Cat No. MP116911100), and by bead beat for 2×30 s (BioSpec). Residual genomic DNA was removed suing Ambion DNase (Thermo Fisher Scientific). cDNA was synthesized using iScript cDNA synthesis kit (Bio-Rad). Real-time quantitative PCR (RT-qPCR) was performed according to Raymond et al. (2020) using the SensiFast SYBR green Hi-ROX One-Step Kit (Bioline). Primers used in this study (Table S3) were designed using PrimerQuest Tool (https://www.idtdna.com/Primerquest/Home/Index).. Relative gene expression was determined on a Bio-Rad CFX Connect Real-Time thermal cycling using the delta-delta Ct method ($2^{-\Delta\Delta CT}$). Histone H2B and 40S ribosomal protein S10 (rps10) were used as reference genes which were previously determined to exhibit stable expression in UWO241 (Raymond et al. 2020).

Statistical Analyses

Statistical significance was determined using Student's paired t-test, uneven variance (OriginPro 8.5.1) between stress conditions and control within a single organism as well as between stress conditions in both organisms. Statistical significance was accepted when P value was less than 0.05.

Results

Growth physiology and PSII photochemistry

To compare the long-term acclimation mechanisms between the psychrophilic UWO 241 and the mesophilic SAG 49.72, the two strains were grown under control growth conditions and then shifted to one of three different treatments, representing high light (HL), low temperature (LT) and high salt (HS) (Table 1). First, it was confirmed that both strains exhibited full acclimation to each long-term treatment by exhibiting log-phase growth and high photochemical activity in mid-log phase cultures. UWO 241 and SAG 49.72 exhibited exponential growth and high PSII photochemical efficiency (F_V/F_M) under all treatments (Fig. S1; Table 2).

Even though UWO 241 tolerates significantly lower temperature and high salinity levels compared with SAG 49.72, the two strains generally exhibited comparable growth rates under control vs. treatment conditions (Table 2). On the other hand, Chl a/b ratios were significantly lower in UWO 241 vs. SAG 49.72 across all growth conditions (Table 2). Moreover, SAG 49.72 cultures grown under all long-term stress conditions exhibited higher Chl a/b ratios compared with control cultures; although, this difference was only significant between the control and low temperature-grown cultures (Table 2). Both organisms exhibited qL values > 0.70 under control vs. treatment, with the exception of HL-cultures which exhibited lower qL in both species relative to controls (Table 2). Steady state NPQ levels remained low in both algal species under LT or HS, while HL-treated cells exhibited a 24- and 7.5-fold increase in NPQ in UWO 241 and SAG 49.72, respectively (Table 2).

77 K Chl a fluorescence emission spectra

77 K emission spectra of whole cells of the mesophilic SAG 49.72 exhibited prominent fluorescence peaks at 684 nm and 714–716 nm consistent with LHCII-PSII and PSI fluorescence emission, respectively (Fig. 1a). In contrast with the mesophile, UWO 241 exhibited major Chl

Table 2 Growth physiology parameters in cultures of UWO 241 and SAG 49.72 grown under control versus long-term stress conditions

Growth condition	Doubling time (h)	F_V/F_M	qL	NPQ	Total chlorophyll (μg ml^{-1})	Chl a/b
UWO 241						
C	49.30 ± 3.80	0.67 ± 0.02[b]	0.72 ± 0.08[b]	0.02 ± 0.04	6.99 ± 1.09	1.00 ± 0.02[b]
HL	43.13 ± 4.14	0.60 ± 0.01[a]	0.60 ± 0.05[b]	0.48 ± 0.15[a,b]	4.02 ± 0.45[a,b]	0.80 ± 0.14[b]
LT	111.7 ± 6.75	0.55 ± 0.02[a,b]	0.82 ± 0.04[b]	0.09 ± 0.08	4.79 ± 0.59[a]	0.97 ± 0.10[b]
HS	35.15 ± 1.62	0.60 ± 0.05[b]	0.70 ± 0.10[b]	0.16 ± 0.04 [a,b]	5.06 ± 0.46	0.90 ± 0.10[b]
SAG 49.72						
C	29.74 ± 3.79	0.70 ± 0.02	0.94 ± 0.04	0.02 ± 0.00	9.26 ± 1.62	2.28 ± 0.77
HL	11.82 ± 3.60	0.65 ± 0.04	0.24 ± 0.00[a]	0.15 ± 0.03 [a]	6.86 ± 0.08	4.29 ± 0.29[a]
LT	39.12 ± 2.77	0.66 ± 0.01[a]	1.00 ± 0.00	0.01 ± 0.01	4.31 ± 0.15 [a]	5.66 ± 0.29[a]
HS	43.15 ± 3.58[a]	0.66 ± 0.04	0.94 ± 0.09	0.04 ± 0.02	8.13 ± 0.84	3.51 ± 0.05

Values are means with standard deviations ($n = 3$ biological replicates)

F_V/F_M maximum photochemical efficiency; *qL* photochemical quenching

[a]Statistical significance between control vs. stress within one algal species

[b]Statistical significance between UWO 241 vs. SAG 49.72 when grown under same treatment ($p < 0.05$)

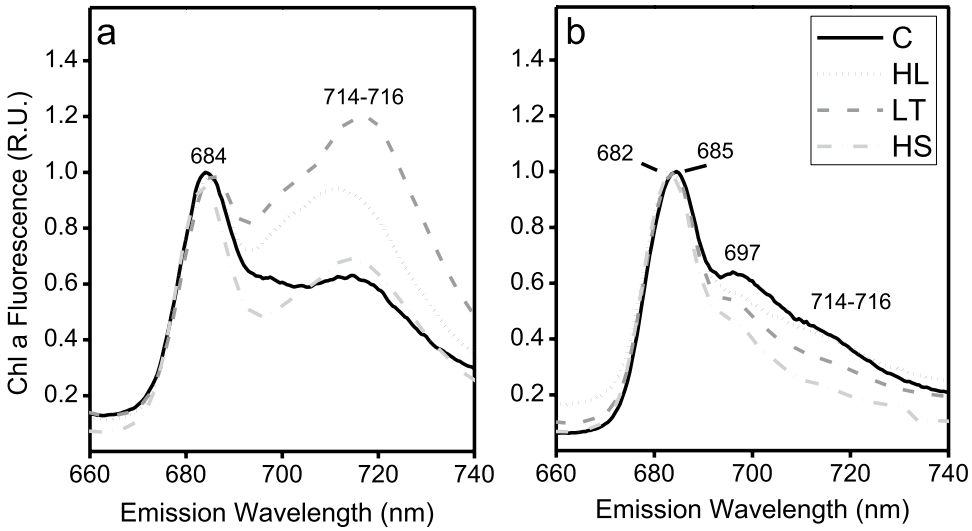

Fig. 1 77 K Chlorophyll a fluorescence emission spectra of the mesophile SAG 49.72 (**a**) and the psychrophile UWO 241 (**b**) acclimated to control and long-term stress conditions. *C* control; *HL* high light; *LT* low temperature; *HS* high salt. See Table 1 for long-term conditions

a fluorescence emission peaks at 685 nm and 697 nm but lacked a prominent emission peak for PSI at longer wavelengths 715–720 nm (Fig. 1b). Acclimation to long-term stress resulted in significant changes in the 77 K Chl a fluorescence emission spectra of SAG 49.72 (Fig. 1a). Gaussian analysis of the fluorescence spectra revealed that SAG 49.72 exhibited a 1.5- to 3.2-fold decrease in the ratio of PSII/PSI fluorescence in response to LT, HL or HS (Table S4). In contrast with stress-acclimated cells of SAG 49.72, UWO 241 cells exhibited minimal changes in PSI fluorescence (Fig. 1b), and only HS resulted in a minor decrease (1.18-fold relative to control) in the PSII/PSI ratio of UWO 241 (Table S4).

Photosystem I activity

PSI activity was monitored in mid-log cultures of both strains acclimated to control or treatments by far red (FR) light inducible P700 photooxidation (Fig. 2). The rise in absorbance at 820 nm (ΔA_{820}) is a relative measure of the fraction of photooxidizable P700 reaction centers, while rates of P700 re-reduction in the dark ($t_{½}^{red}$) reflect electron donation from alternative donors and mainly CEF (Ivanov et al. 1998). UWO 241 exhibited significantly lower FR-inducible ΔA_{820} compared to SAG 49.72 under both control and stress-acclimated conditions (Fig. 2a). UWO 241 cells grown in control or stress-acclimated conditions exhibited significantly faster $t_{½}^{red}$ compared with SAG 49.72 grown under all conditions, suggesting that UWO 241 exhibited

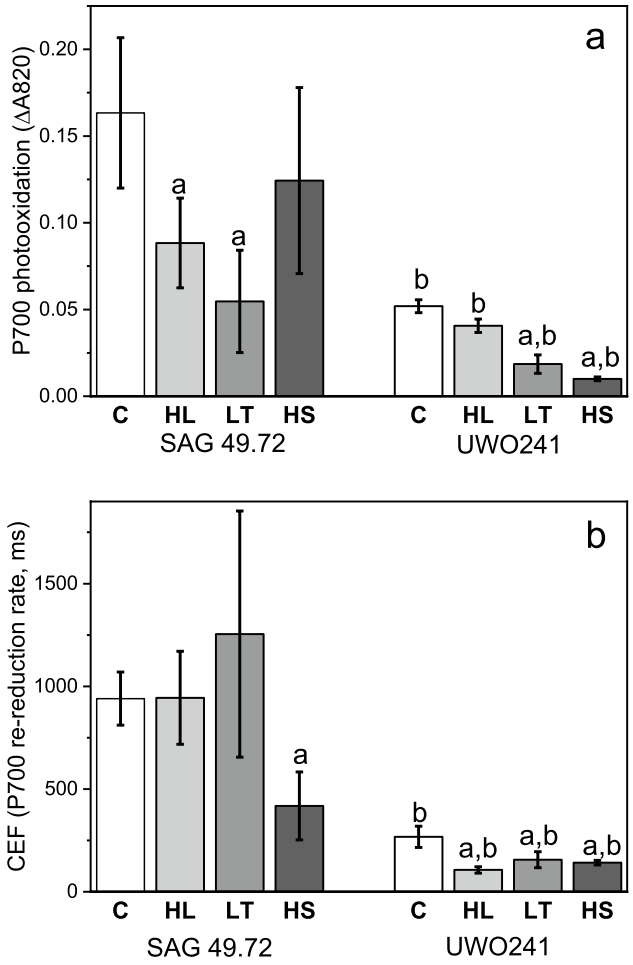

Fig. 2 Photosystem I (P700) oxidation/reduction of the mesophile SAG 49.72 and the psychrophile UWO 241 grown under control and long-term stress conditions. **a** Oxidation state of P_{700}. **b** Re-reduction kinetics of P_{700}^{+}. P_{700} oxidation/reduction was monitored in the presence of far red light. Letters—a, statistical significance between control vs. stress within one algal species; b, statistical significance between UWO 241 vs. SAG 49.72 when grown under same treatment ($n=3$; $p<0.05$). *C* control; *HL* high light; *LT* low temperature; *HS* high salt. See Table 1 for long-term conditions

constitutively higher rates of CEF (Fig. 2b). Furthermore, $t_{½}^{red}$ was also significantly faster in stress-acclimated versus control cultures of UWO 241 (Figs. 2b and S2). These results agreed with a recent report which compared P700 photooxidation with electrochromic shift measurements to show that UWO 241 possesses increased CEF under high salt versus low salt conditions (Kalra et al. 2020).

Relationship between NPQ and CEF

We measured the capacity for NPQ under a range of measuring irradiance levels. The mesophilic strain SAG 49.72 maintained low NPQ levels over the range of irradiance levels under all conditions (Fig. 3). In contrast, control UWO

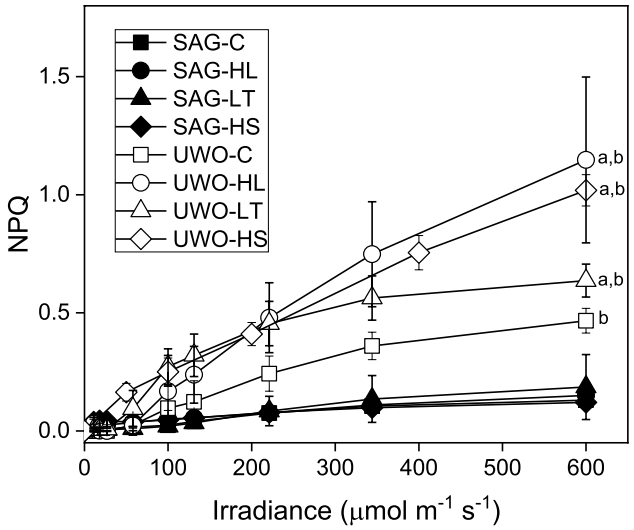

Fig. 3 Capacity for nonphotochemical quenching in UWO 241 (UWO) and SAG 49.72 (SAG) grown under control and long-term stress conditions. Letters—a, statistical significance between control vs. stress within one algal species; b, statistical significance between UWO 241 vs. SAG 49.72 when grown under same treatment ($n=3$; $p<0.05$). *C* control; *HL* high light; *LT* low temperature; *HS* high salt. See Table 1 for long-term conditions

241 cells exhibited significantly higher NPQ compared with that of SAG 49.72. Furthermore, stress acclimation in UWO 241 resulted in a further increase in NPQ capacity; however, with HL- and HS-UWO 241 exhibiting higher maximum NPQ relative to LT-UWO 241 cultures (Fig. 3).

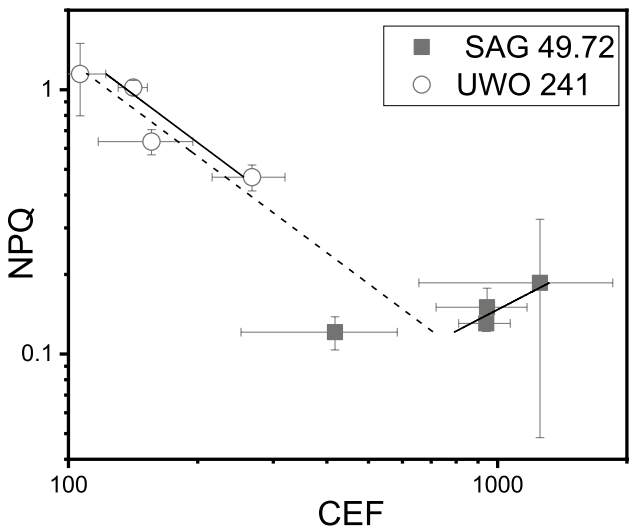

Fig. 4 NPQ and CEF exhibit a linear relationship. SAG 49.72 and UWO241 grown under control and long-term stress conditions. NPQ axis represents maximum NPQ values determined from light response curves in Fig. 3. CEF represents P_{700}^{+} re-reduction rates. Dashed and solid lines show linear regression for all data points or individual organisms, respectively ($n=3$ or 7–9 for NPQ and CEF, respectively)

Next, we determined whether high CEF was associated with a stronger capacity for NPQ (Fig. 4). All UWO 241 cultures exhibited faster rates of CEF and higher maximum NPQ levels relative to SAG 49.72. A strong negative correlation was observed between NPQ capacity and CEF within either the dataset across all experiments or within UWO 241 samples ($r^2 = 0.93$ and 0.99, respectively). In contrast, SAG 49.72 exhibited a weak positive correlation between NPQ and CEF ($r^2 = 0.52$).

Expression of key NPQ, CEF genes

We monitored expression of several key genes of photosynthesis, NPQ and CEF in cells of UWO 241 grown under either control or long-term stress (Fig. 5). Gene expression of major reaction center proteins *psbA* and *psaA* were generally comparable to or lower in the treatments relative to control cultures (Fig. 5a,b). Since all stress treatments resulted in a higher capacity for NPQ in UWO 241, we searched the UWO 241 genome and transcriptome for LhcSR homologues, which are essential for NPQ in green algae (Maruyama et al. 2014; Peers et al. 2009). We identified several potential LhcSR homologues in the UWO 241genome (Accession numbers KAG1678527, KAG1678528, KAG1678497 and KAG1678500), two of which (KAG1678527 and KAG1678528; LhcSR1.1 and LhcSR2.1, respectively) were also expressed in the transcriptome (Fig. S3). We designed qPCR primers for LhcSR1.1 and LhcSR2.1 (Table S3) and monitored their expression in UWO 241 cultures grown under control and

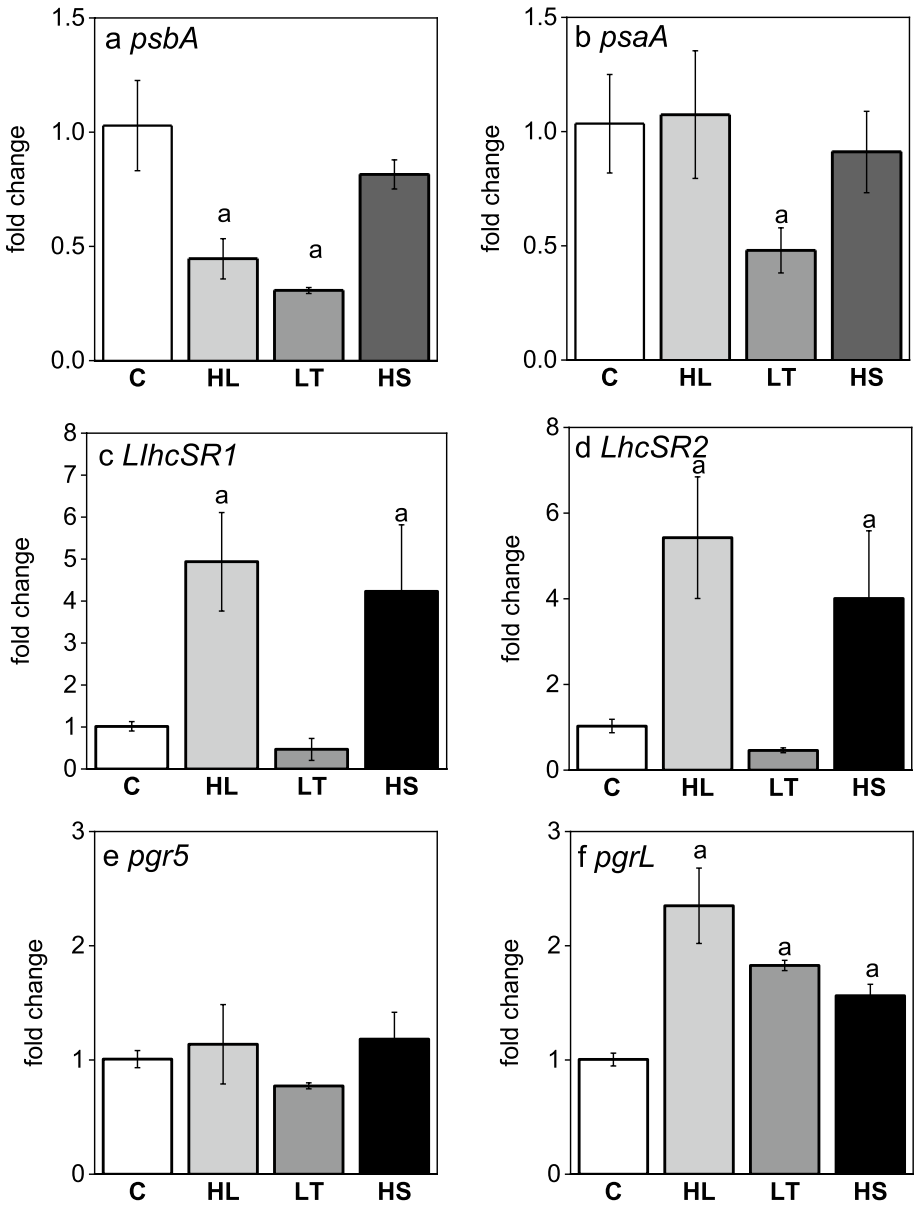

Fig. 5 Transcript levels of several key genes in UWO 241 grown under control and long-term stress conditions. Expression levels were determined by RT-qPCR. **a** Statistical significance between control vs. stress ($n = 4$; $p < 0.05$). *C* control; *HL* high light; *LT* low temperature; *HS* high salt. See Table 1 for long-term conditions

long-term stress conditions. Expression of both LhcSRs was upregulated 3.5- and fourfold in HL- and HS-UWO 241, respectively, relative to control. In contrast, LhcSR expression in the LT-UWO 241 cultures was comparable with the control (Fig. 5c, d).

We also identified homologues of the proton gradient regulation genes *pgr5* and *pgrL* in both the genome and the transcriptome of UWO 241 (Accession Numbers KAG1678016 and KAG1672779, respectively). We designed qPCR primers for both genes (Table S3) and monitored their expression in UWO 241 cultures grown under all four conditions. Expression of *pgr5* was comparable across all three treatments and the control cultures. Relative to control, *pgrL* expression was significantly upregulated in all three treatments, with HL-UWO 241 cells exhibiting the highest increase in expression relative to control conditions (2.35-fold; Fig. 5 e, f).

Antioxidant response

We monitored the capacity of UWO 241 and SAG 49.72 to avoid ROS accumulation under short-term stress. Control-grown cultures were exposed to either high light or low temperature stress for up to 1 h and monitored the production of O_2^- (Fig. 6) and H_2O_2 (Figs. S4, S5a). The mesophile SAG 49.72 exhibited significantly higher levels of O_2^- relative to pre-treated cells following either short-term HL or LT treatment. Conversely, UWO 241 exhibited no significant change in levels of either ROS after the short-term stress treatments (Figs. 6 and S4). Last, we used a second assay to compare H_2O_2 levels between UWO 241 and *C. reinhardtii*. Relative to *C. reinhardtii,* UWO 241 exhibited > 200-fold lower levels H_2O_2 both prior to and after the short-term HL treatment (Fig. S5a).

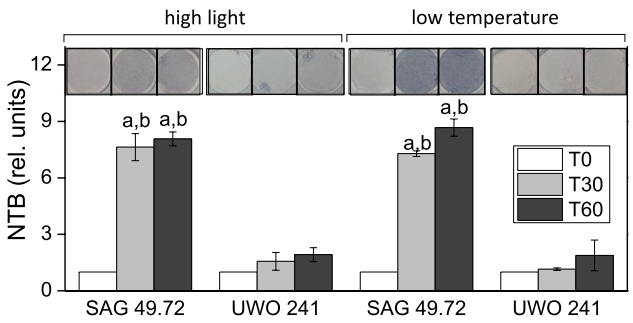

Fig. 6 Production of reactive oxygen species in UWO 241 (P) vs. SAG 49.72 (M) during short-term incubation in low temperature (5 °C) or high light (300 µmol m^{-2} s^{-1}) stress. Algal samples were incubated for 1 h in the presence of NBT dye to detect superoxide. Data is normalized to time 0. Letters—a, statistical significance between control vs. stress within one algal species; b, statistical significance between UWO 241 vs. SAG 49.72 when grown under same treatment ($n = 3$; $p < 0.05$)

The enzymes APX and GR are key enzymes of an ROS detoxification pathway, the AsA-GSH cycle, catalyzing the first step of the pathway and regeneration of reduced glutathione, respectively (Noctor and Foyer 1998). Enzymatic assays revealed low activity for both enzymes in SAG 49.72 grown under control or HL, LT and HS stress conditions (Fig. 7). In contrast, UWO 241 exhibited significantly higher activity for both enzymes under control and all stress treatments relative to SAG 49.72 (Fig. 7). GR activity was highest in HS-UWO 241 cells, while APX activity was highest in LT-UWO 241 cells relative to controls. Last, the major AsA-GSH pathway substrate, ascorbate, was significantly higher in UWO 241 compared with values typically reported

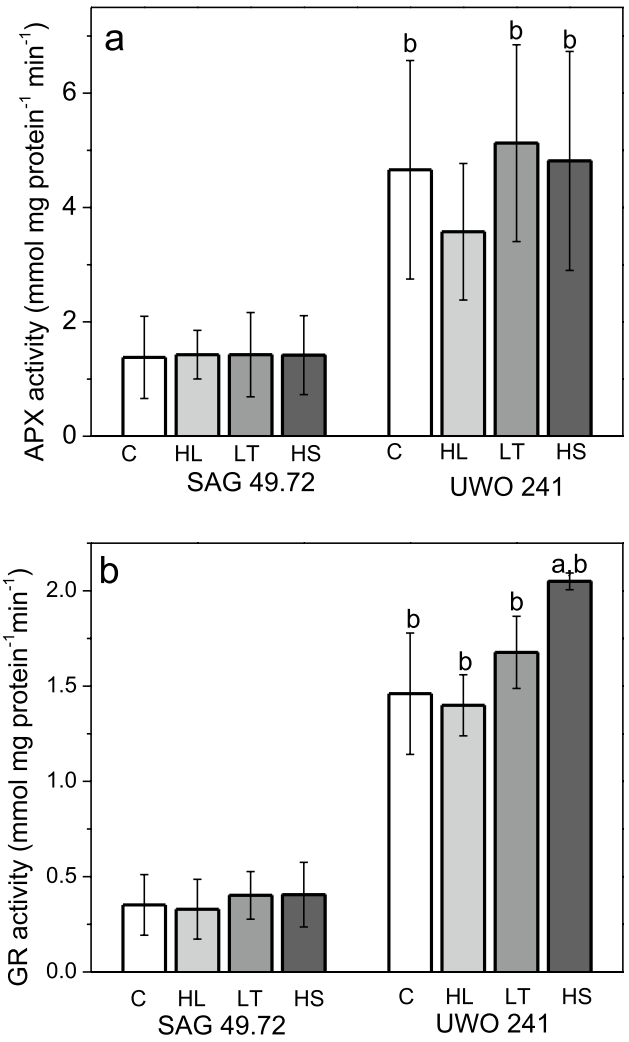

Fig. 7 Activity of AsA-GSH pathway enzymes, ascorbate peroxidase (APX, **a**) and glutathione reductase (GR, **b**) in SAG 49.72 and UWO 241 grown under control and long-term stress conditions. Letters—a, statistical significance between control vs. stress within one algal species; b, statistical significance between UWO 241 vs. SAG 49.72 when grown under same treatment ($n = 3$; $p < 0.05$). *C* control; *HL* high light; *LT* low temperature; *HS* high salt. See Table 1 for long-term conditions

for other algae (Gest et al. 2013). Total cellular ascorbate 9.61 ± 1.20 and 18.52 ± 1.90 mM ascorbate in UWO 241 cells grown under control and HS conditions, respectively, compared with 0.93 ± 0.30 mM in the mesophile, *C. reinhardtii* (Fig. S5b).

In addition to the ascorbate pathway, we checked expression of three other major antioxidant enzymes using qPCR (Fig. 8). Chloroplastic Fe-SOD expression levels were comparable or lower in the treatments relative to control, with the exception of HS-UWO 241 cells which exhibited a 3.3-fold increase. Other antioxidant enzymes (CAT and GPX) exhibited expression levels at or below control levels in all treatments (Fig. 8).

UWO 241 has multiple homologues of AsA-GSH cycle enzymes

Screening of the UWO 241 genome and transcriptome revealed homologs for all genes involved in the AsA-GSH cycle, with the exception of monodehydroascorbate reductase (MDHAR) (Tables S1 and S2). The genome of UWO 241 encodes 5 genes identified as APX (APX1, APX2-A to –D), which share a high sequence similarity with homologous genes from other photosynthetic organisms and the presence of conserved motifs involved in APX catalytic function (Fig. S6a). Four of these genes (APX2-A to –D) are found on the same contig in a head-to-tail orientation and share a high sequence similarity (83.1–93.3%), suggesting a recent gene duplication event (Fig. S6b). This is in contrast with other green algae that typically encode one or two APX genes with confirmed APX activity (Pitsch et al., 2010; Gest et al., 2013). All other genes, including GR, were present as a single copy and shared a high sequence identity with homologous genes from *C. reinhardtii* (Table S2).

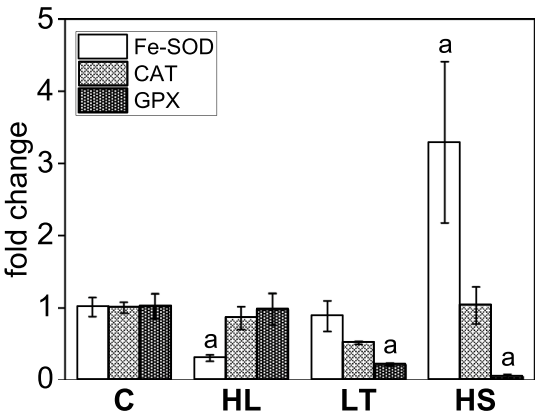

Fig. 8 Transcript levels of genes ROS detoxification genes in UWO241 following acclimation to long-term stress. Expression levels were determined by RT-qPCR. Letters—a, statistical significance between control vs. stress ($n = 4$; $p < 0.05$). *C* control; *HL* high light; *LT* low temperature; *HS* high salt. See Table 1 for long-term conditions

Discussion

This study examined whether two *Chlamydomonas* species adapted to extreme contrasts in their native environments rely upon comparable strategies during acclimation to long-term stress conditions. SAG 49.72 was originally isolated from a temperate lake: it is a mesophilic species and possesses limited ability to acclimate to either salinity or low temperature stress (Szyszka et al. 2007; Pocock et al. 2011). In contrast, in its native Antarctic lake environment, UWO 241 has survived under permanent low temperature and hypersalinity stress for at least 1000 years, based on estimates of the last occurrence of ice-free conditions in Lake Bonney (Morgan-Kiss et al. 2006). Our results confirmed that although both the mesophilic SAG 49.72 and the psychrophilic UWO 241 exhibited the ability to grow under high light, low temperature or high salinity, their tolerance levels and long-term acclimatory strategies are distinct. For the mesophilic SAG 49.72, long-term acclimation can be summarized a reduction in PSII antenna size and energy re-distribution from PSII to PSI, both classic long-term acclimatory mechanisms described for other model algal species (Maxwell et al. 1994; Tanaka and Melis 1997). In contrast, the psychrophilic UWO 241 showed minimal changes in either PSII antenna size or PSII/PSI energy distribution and relies on constitutive PSI-driven CEF and ROS detoxification.

Long-term stress acclimation in the mesophile SAG 49.72 involved an increase in the ratio of Chl a/b and a concomitant decrease in PSII/PSI at the level of 77 K fluorescence emission. Higher Chl a/b ratios in response to long-term stress have been reported across many algae and plants and coincides with a reduction in the size of LHCII (Maxwell et al. 1994; Wilson and Huner 2000; Smith et al. 1990). Reductions in PSII/PSI stoichiometry under either high light or low temperature stress reflect re-distribution of absorbed light energy from PSII to PSI (Smith et al. 1990; Velitchkova et al. 2020). UWO 241 does not appear to rely on either of these classic acclimatory mechanisms to survive long-term stress. Morgan-Kiss et al. (2002b) demonstrated that UWO 241 is also unable to undergo state transitions, exhibiting minimal phosphorylation of light harvesting antenna proteins. More recently, Szyszka-Mroz and colleagues suggested that the psychrophile relies instead on spill-over mechanism under HS growth conditions (Szyszka-Mroz et al. 2019). Thus, UWO 241 is a natural variant lacking state transitions that maintains a relatively large LHCII and high PSII content

under long-term stress. Despite the apparent deficiency of some acclimatory mechanisms common model species, acclimated UWO 241 cells maintained a high qL and comparable energy partitioning relative to control conditions. These results suggest that the psychrophile may use alternative processes to avoid high excitation pressure and increased risk of photooxidative stress.

PSI-driven CEF is an essential process in plants and algae for energy balance and photoprotection (Kramer and Evans 2011; Lucker and Kramer, 2013; Kukuczka et al. 2014); although, most studies of CEF have been restricted to short-term stress exposure (Iwai et al. 2010; Takahashi et al. 2013; Strand et al. 2015). Early reports identified that UWO 241 exhibits relatively high rates of PSI-driven CEF compared with mesophilic strains (Morgan-Kiss et al. 2002b, 2006; Szyszka et al. 2007). Maximal CEF requires restructuring of the UWO 241 photosynthetic apparatus and assembly of a novel PSI supercomplex (Kalra et al. 2020; Szyszka-Mroz et al. 2015). The UWO 241 supercomplex is distinct from that of previously described complex from *C. reinhardtii* (Iwai et al. 2010) because the former is not associated with state-transition-inducing treatments and it lacks typical PSI 77 K fluorescence emission despite the presence of many PSI core proteins (Kalra et al. 2020; Szyszka-Mroz et al. 2015). Here we show that UWO 241 exhibits faster CEF rates under not only high salinity, but also high light and low temperatures, suggesting that this extremophile relies on CEF as a general long-term acclimatory strategy. The proteins PGR5 and PGRL1 have been implicated in CEF and formation of PSI supercomplexes (DalCorso et al. 2008; Hertle et al. 2013; Kukuczka et al. 2014). All UWO 241 cultures acclimated to long-term stress showed an increase in PGRL1 but not PGR5 expression. A PGR5 Like-1 protein was also detected in the PSI supercomplex of UWO 241; however, PGR5 but not PGRL1 were upregulated in HS-UWO 241 whole cell proteomes (Kalra et al. 2020). Cook et al. (2019) found that PGRL protein levels were down-regulated in UWO 241 cultures grown in high iron which corresponded to a slower CEF in high Fe-grown cultures. Thus, it appears that PGRL1 is a probable candidate of the CEF mechanism or PSI supercomplex in UWO 241; however, more research is required to clarify the roles of the PGR proteins.

CEF generates additional transthylakoid pmf which can be utilized for several purposes, including balancing ATP/NADPH production and photoprotection of both PSII and PSI (Bulte et al. 1990; He et al. 2015; Chaux et al. 2015; Lucker and Kramer 2013; Yamori et al. 2016). Kalra and colleagues showed that under long-term HS stress CEF serves multiple purposes in UWO 241, including additional ATP production as well as constitutive photoprotection (Kalra et al. 2020). Higher ATP levels are used in part to support enhanced CBB pathway activity which supplies substrates for storage compounds (starch), osmoregulants (glycerol), as well as the shikimate pathway (Kalra et al. 2020). It is likely that CEF is utilized for similar processes when UWO 241 is acclimated to HL or LT. This current study provides evidence that high CEF in all three treatments is associated with enhanced photoprotection of PSII. Increased CEF rates in cells of UWO 241 acclimated to HL, LT or HS all exhibited a higher capacity for NPQ compared with control cells. Unlike the mesophilic SAG 49.72, NPQ capacity and CEF levels were strongly correlated in the psychrophilic UWO 241 (Fig. 4). These results suggest a constitutive capacity for PSII protection which is likely due to enhanced CEF-generated pmf.

There is recent evidence that activation of CEF and NPQ are common acclimation strategies among high latitude phytoplankton communities (Young and Schmidt 2020). A second Lake Bonney chlorophyte, *Chlamydomonas* sp. ICE-MDV, exhibited comparably fast CEF rates as UWO 241, which were further increased under Fe-stress (Cook et al 2019). The snow alga, *Chlamydomonas nivalis*, increased CEF under low temperature stress (Zheng et al. 2020). Similar to our findings, enhanced CEF in the snow alga was accompanied by activation of NPQ and antioxidant activity (Zheng et al. 2020). High NPQ has also been detected in phytoplankton communities in the Arctic sea ice (Galindo et al. 2017), and there are alternative NPQ mechanisms described in Arctic Prasinophytes (Liefer et al. 2018) and Southern Ocean diatoms (Strzepek et al. 2019).

In green algae, efficient induction of NPQ is dependent upon expression of one or more LHCSRs (Maruyama et al. 2014; Peers et al. 2009). A previous study on acclimation to iron availability in UWO 241 detected upregulation of LHCSR1 under excess Fe conditions (Cook et al. 2019). More recently, Kalra et al. (2020) detected LHCSR1 in several chlorophyll protein complexes isolated from HS-grown UWO 241. In this current work, we detected four possible LHCR homologues in the UWO 241 genome: transcripts of two (*LhcSR*1 and *LhcSR*2) were also detected in a transcriptome. No homologues were found for the third LHCSR, *lhcsr*3, which along with LHCSR1 has been shown to be important for thermal dissipation in both PSII and PSI (Girolomoni et al. 2019). Another related Antarctic green alga, *Chlamydomonas* sp. ICE-L expresses *LhcSR1* and *LhcSR2* in response to either UV-B radiation or high salt, but LhcSR3 was not detected in this psychrophilic alga either (Mou et al. 2012). The primitive plant *Physcomitrella* also expresses only *LhcSR1* and *LhcSR2* in addition to the plant *psbS* (Alboresi et al. 2010). In this current student, expression of both *LhcSR*s were upregulated in the HL- and HS-UWO 241 cultures relative to controls; however, transcript levels in LT-grown cells were not different from controls. These data fit well with the NPQ capacity of UWO 241 which was highest in HL and HS conditions.

CEF contributes to PSI photoprotection by preventing acceptor-side limitation of PSI electron flow (Huang et al. 2009). Over-reduction of PSI manifests as production of the ROS, O_2^- (Asada 1999). We show that UWO 241 possesses remarkable ability to avoid O_2^- accumulation: cells exposed to either short-term LT or HL stress exhibited minimal accumulation of this ROS. This ability to keep O_2^- levels lows is in part due to CEF-associated prevention of PSI acceptor side limitation. In contrast, SAG 49.72 exhibited significant levels of O_2^- when exposed to the same conditions. While PSII is typically considered sensitive to all environmental stresses, PSI photodamage occurs under specific environmental conditions, including drought, high salinity and low temperature, and repair of PSI is slow and inefficient (Huang et al. 2012, 2016, 2017; Yamori et al. 2016; Ivanov et al. 1998; Zhang and Scheller 2004). Thus, PSI photoinhibition can have a serious consequence for survival under long-term stress. We suggest that constitutive CEF simultaneously plays critical roles in protecting both PSII and PSI from photodamage in UWO 241 for survival under long-term environmental stress.

UWO 241 exhibits constitutive protection of PSII and PSI by minimizing ROS production; however, there is also evidence that the psychrophile possesses enhanced ability for ROS detoxification. The AsA-GSH pathway is a major ROS detoxification pathway in plants and is responsible for regeneration of the antioxidant ascorbate (Foyer and Shigeoka 2011; Foyer and Noctor 2012). The AsA-GSH pathway involves four enzymes, ascorbate peroxidase (APX), monohydroascorbate reductase (MDHAR), dehydroascorbate reductase (DHAR), and glutathione reductase (GR) (Noctor and Foyer 1998). Plants express multiple isoforms of each enzyme, in particular APX (Pitsch et al. 2010; Teixeira et al. 2004). High concentrations of ascorbate accumulate in plants, particularly under stress conditions, including high light, low temperatures and high salinity (Bartoli et al. 2017; Maruta and Ishikawa 2017; Wildi and Lütz 1996; Zechmann et al. 2011; Zhang et al. 2011). On the other hand, cyanobacteria and algae exhibit significantly lower levels of ascorbate and possess only one isoform or are missing one or more enzymes of the AsA-GSH pathway (Gest et al. 2013). For example, the model *C. reinhardtii* appears to lack the thylakoid-bound APX found in plants, expressing only a single isoform of APX which is localized to the stroma (Pitsch et al. 2010). A second APX2 isoform has been predicted to localize to the chloroplast, but its function has not been studied (Wu and Wang, 2019). Three pieces of evidence indicate that UWO 241 may rely on the AsA-GSH pathway to a greater extent than previously appreciated in other algal species. First, activity of two enzymes, APX and GR, are constitutively high in UWO 241 relative to the mesophile SAG 49.72 under both control and all long-term stress conditions. Second, UWO 241 cells accumulated millimolar levels of the substrate ascorbate, which is atypically high compared to algal strains (Gest et al. 2013), which was correlated with extremely low levels of the ROS stubstrate of the AsA-GSH pathway, H_2O_2 (Fig. S5). Last, unlike other algae studied thus far, UWO 241 appears to possess more isoforms of several enzymes necessary for ascorbate cycling. A search of a previously published transcriptome of UWO 241 (Raymond and Morgan-Kiss 2013) revealed multiple potential homologues for enzymes of the AsA pathway, including 3 APX, 3 DHAR, and 3 GR genes (Tables S1 and S2). These genes were also detected at the level of the genome, with four APX genes present as highly similar tandem duplicates (Fig. S6). In addition, one of the putative UWO 241 APX proteins is related to a plant thylakoid-bound isoform from *Triticum aestivum*. APX catalyzes the oxidation of ascorbate by H_2O_2, while DHAR and GR work in concert to regenerate glutathione. We did not identify an isoform for MDHAR in the genome or transcriptome, which is needed for recycling of ascorbate. The additional isoforms may be localized to different cellular compartments, as in plants, or may contribute to constitutively high AsA-GSH pathway activity. Gene duplications have been shown for several other UWO 241 genes including photosynthetic ferredoxin (Cvetkovska et al. 2018), chlorophyllide a oxygenase (Cvetkovska et al. 2019) and the chloroplast kinase Stl-1 (Szyszka-Mroz et al., 2019).

We propose an updated model for the psychrophilic halophyte, *C.* sp. UWO241 which allows this extremophile to acclimate to a range of long-term stress conditions (Fig. 9). As an adaptation to extreme shade conditions, UWO241 maintains a large LHCII antenna, regardless of its growth condition (Morgan et al. 1998; Szyska et al. 2007), while LHCI is apparently permanently downregulated (Morgan et al. 1998; Kalra et al. 2020; Fig. 9). A recent paper suggested that energy is shared between the two photosystems through a poorly understood spill-over mechanism (Szyska-Mroz et al. 2019); although, in an earlier report, it was suggested that PSI and PSII are relatively distant from each other compared with *C. reinhardtii* (Morgan-Kiss et al. 2002a, 2002b). Regardless of the status of exciton energy sharing between the photosystems, CEF is a central in this alga's acclimation mechanism (Fig. 9, ②). High rates of CEF provide multiple opportunities for aiding in survival and growth under long-term stress. First, there is for photoprotection of both photosystems, through LHSR-mediated NPQ at PSII (Fig. 9, ③) and avoidance of acceptor-side limitation at PSI. Second, high rates of CEF also provide the organism with the option of additional ATP production for maintaining energy balance (Kalra et al. 2020). A bestrophin-like protein dissipates CEF-generated membrane potential ($\Delta\psi$) through Cl- influx into the lumen, supporting sustained high transthylakoid ΔpH (Cook et al. 2019; Fig. 9, ④). Despite this robust system of constitutive photoprotection which should minimize ROS

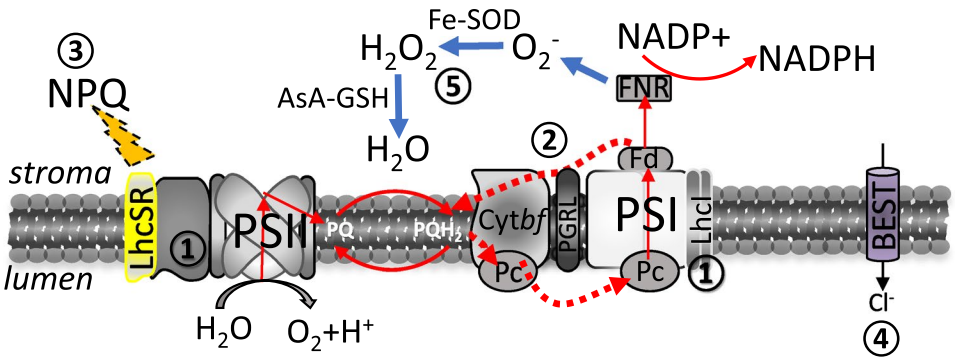

Fig. 9 Model of long-term acclimation strategies which allow the psychrophilic halophyte, *Chlamydomonas* sp. UWO241 to maintain efficient photosynthesis and growth under growth conditions which are nonpermissible for model organisms such as *C. reinhardtii*. The model integrates discoveries made in this current work as well as additional findings from earlier publications. (1) Maintenance of a large LHCII and a permanently downregulated LHCI antennae as a consequence of adaptation to extreme shade/blue light (this study; Morgan et al. 1998; Szyzska et al. 2007), (2) efficient nonphotochemical quenching capacity mediated by LHCSRs (this study), (3) high rates of PSI-driven cyclic electron flow mediated by the PGRL1 pathway within a PSI supercomplex for excitation energy balance and ATP production (this study; Szyska-Mroz et al. 2015; Kalra et al. 2020), (4) Bestrophin-like ion channels transports anions into the lumen to dissipate high electrical potential caused by CEF-driven high trans-thylakoid pmf (Cook et al. 2019), (5) high capacity for ROS detoxification through Fe-SOD and the Ascorbate–Glutathione pathway (this study)

production, UWO 241 also relies on redundant pathways of ROS detoxification to ensure tight control over ROS levels (Fig. 9, ⑤).

Conclusions and renaming of UWO 241

This study builds upon more than two decades of work on the enigmatic, Antarctic alga, *Chlamydomonas* sp. UWO 241 which have documented novel adaptation strategies to survive permanent extreme conditions. Over the years, the taxonomic identity of UWO 241 has experienced much change: originally identified on a morphological basis in 1995 as *C. subcaudata* by J. Priscu (Neale & Priscu 1995), the organism was erroneously renamed in 2004 as *C. raudensis* UWO 241 (Pocock 2004). Recently, a thorough revisiting on the taxonomy of the strain performed by Possmayer et al. (2016) concluded that UWO 241 represents a unique lineage within the Moewusinia clade, and it was therefore renamed *Chlamydomonas* sp. UWO 241 as a place holder name. Molecular phylogenetic analysis of the full length 18S rRNA gene revealed that the closest known relative of UWO 241 is a marine alga, *Chlamydomonas parkeae* SAG 24.89 (95% identity). Furthermore, a recent report revealed that the genome of UWO 241 is relatively large (212 Mb) and features several novel characteristics, including hundreds of duplicated genes (Zhang et al. 2021). Given its geographical isolation and unique physiology, combined with recent molecular and genomic analyses, we suggest that UWO 241 is a unique strain. According to requirements of the International Code of Nomenclature for algae, fungi, and plants (McNeill et al. 2012) we propose to rename the strain *Chlamydomonas priscuii* in recognition of John C. Priscu, the investigator who originally isolated the strain in 1995 (Neale and Priscu 1995).

Supplementary Information The online version contains supplementary material available at https://doi.org/10.1007/s11120-021-00877-5.

Acknowledgements The authors thank Prof. John C. Priscu (Montana State University) for isolation and donation of the algal strain *Chlamydomonas* sp. UWO 241 (originally named *Chlamydomonas subcaudata*) from Lake Bonney, McMurdo Dry Valleys, Antarctica. RMK, SS-R, and MH were supported by the National Science Foundation, Office of Polar Programs under Award #OPP-1056396 (growth physiology, photoinhibition, antioxidant measurements). IK, SD and DP were supported by the U.S. Department of Energy (DOE), Office of Science, Basic Energy Sciences (BES) under award #DE-SC0019138 (PSI, CEF measurements). MC was supported by a National Sciences and Engineering Research Council of Canada (NSERC) Discovery Grant RGPIN-2019-05763 and University of Ottawa start-up funding (genome screening).

Author contributions SS-R and RMK conceptualized the research; SS-R, SD, IK, MH, DP, and MC performed the investigations; SS-R, RMK, and MH developed the methodology; SS-R, RMK and MC performed data curation; RMK provided project administration; RMK and MC helped with funding acquisition; SS-R and RMK wrote the original draft of the manuscript; SD, IK, MH, and MC reviewed and edited the manuscript.

Funding RMK, SS-R, and MH were supported by the National Science Foundation, Office of Polar Programs under Award #OPP-1056396 (growth physiology, photoinhibition, antioxidant measurements). IK, SD and DP were supported by the U.S. Department of Energy (DOE), Office of Science, Basic Energy Sciences (BES) under Award #DE-SC0019138 (PSI, CEF, H_2O_2 measurements). MC is supported by a National Sciences and Engineering Research Council of Canada

(NSERC) Discovery Grant RGPIN-2019–05763 and University of Ottawa start-up funding (genome screening).

Availability of data and material The data supporting the findings of this study are available from the corresponding author (RMK) upon request.Code availability Not applicable.

Code availability Not applicable.

Declarations

Conflict of interest All authors declare that they have no conflict of interest.

References

Alboresi A, Gerotto C, Giacometti GM, Bassi R, Morosinotto T (2010) *Physcomitrella patens* mutants affected on heat dissipation clarify the evolution of photoprotection mechanisms upon land colonization. Proc Natl Acad Sci 107:11128–11133

Aldesuquy HS, Baka ZA, El-Shehaby O, Ghanem HE (2013) Growth, lipid peroxidation and antioxidant enzyme activities as a selection criterion for the salt tolerance of wheat cultivars irrigated by seawater. Phyton 53:153–165

Apel K, Hirt H (2004) Reactive oxygen species: Metabolism, oxidative stress, and signal transduction. Annu Rev Plant Biol 55:373–399

Asada K (1996) In: Baker NR (ed) Photosynthesis and the Environment. Springer, Berlin, p 123

Asada K (1999) The water-water cycle in chloroplasts: scavenging of active oxygens and dissipation of excess photon. Annu Rev Plant Physiol Plant Mol Biol 50:601–639

Asada K (2000) The water-water cycle as alternative photon and electron sinks. Philos Trans R Soc Lond B Biol Sci 355(1402):1419–1431

Asada K (2006) Production and scavenging of reactive oxygen species in chloroplasts and their functions. Plant Physiol 141(2):391–396

Bartels D, Sunkar R (2005) Drought and salt tolerance in plants. Crit Rev Plant Sci 24(1):23–58

Bartoli CG, Buet A, Grozeff GG, Galatro A, Simontacchi M (2017) Ascorbate-glutathione cycle and abiotic stress tolerance in plants. In: Hossain MA (ed) Ascorbic acid in plant growth, development and stress tolerance. Springer, Berlin, pp 177–200

Borowitzka MA (2018) The 'stress' concept in microalgal biology—homeostasis, acclimation and adaptation. J Appl Phycol 30:2815–2825

Bulte L, Gans P, Febeille F, Wollman F (1990) ATP control on state transitions in vivo in *Chlamydomonas reinhardtii*. Biochem Biophys Acta 1020:72–80

Chaux F, Peltier G, Johnson X (2015) A security network in PSI photoprotection: regulation of photosynthetic control, NPQ and O_2 photoreduction by cyclic electron flow. Front Plant Sci 6:875

Chen Q, Zhang M, Shen S (2011) Effect of salt on malondialdehyde and antioxidant enzymes in seedling roots of Jerusalem artichoke (*Helianthus tuberosus* L.). Acta Physiol Plant 33(2):273–278

Cook G, Teufel A, Kalra I, Li W, Wang X, Priscu J, Morgan-Kiss R (2019) The antarctic psychrophiles *Chlamydomonas* spp. UWO241 and ICE-MDV exhibit differential restructuring of photosystem I in response to iron. Photosynth Res 141:209–228

Cournac L, Latouche G, Cerovic Z, Redding K, Ravenel J, Peltier G (2002) In vivo interactions between photosynthesis, mitorespiration, and chlororespiration in *Chlamydomonas reinhardtii*. Plant Physiol 129(4):1921–1928

Cvetkovska M, Hüner NP, Smith DR (2017) Chilling out: the evolution and diversification of psychrophilic algae with a focus on Chlamydomonadales. Polar Biol 40:1169–1184

Cvetkovska M, Orgnero S, Hüner NP, Smith DR (2019) The enigmatic loss of light-independent chlorophyll biosynthesis from an Antarctic green alga in a light-limited environment. New Phytol 222(2):651–656

DalCorso G, Pesaresi P, Masiero S, Aseeva E, Schünemann D, Finazzi G, Joliot P, Barbato R, Leister D (2008) A complex containing PGRL1 and PGR5 is involved in the switch between linear and cyclic electron flow in *Arabidopsis*. Cell 132:273–285

Ensminger I, Busch F, Hüner NPA (2006) Photostasis and cold acclimation: sensing low temperature through photosynthesis. Physiol Plant 126(1):28–44. https://doi.org/10.1111/j.1399-3054.2006.00627.x

Falk S, Krol M, Maxwell DP, Rezansoff DA, Gray GR, Hüner NPA (1994) Changes in in vivo fluorescence quenching in rye and barley as a function of reduced PSII light harvesting antenna size. Physiol Plant 91:551–558

Falk S, Maxwell D, Gray G, Rezansoff D, Hüner N (1993) Photosynthetic acclimation to low temperature in higher plants and algae. Curr Top Bot Res 1:281–292

Förster B, Osmond CB, Pogson BJ (2005) Improved survival of very high light and oxidative stress is conferred by spontaneous gain-of-function mutations in *Chlamydomonas*. Biochim Et Biophys Acta-Bioenerg 1709(1):45–57

Foyer CH, Halliwell B (1976) The presence of glutathione and glutathione reductase in chloroplasts: a proposed role in ascorbic acid metabolism. Planta 133(1):21–25

Foyer CH, Lopez-Delgado H, Dat JF, Scott IM (1997) Hydrogen peroxide-and glutathione-associated mechanisms of acclimatory stress tolerance and signalling. Physiol Plant 100(2):241–254

Foyer CH, Noctor G (2012) Managing the cellular redox hub in photosynthetic organisms. Plant Cell Environ 35(2):199–201

Foyer CH, Shigeoka S (2011) Understanding oxidative stress and antioxidant functions to enhance photosynthesis. Plant Physiol 155(1):93–100

Galindo V, Gosselin M, Lavaud J, Mundy CJ, Else B, Ehn J, Babin M, Rysgaard S (2017) Pigment composition and photoprotection of Arctic sea ice algae during spring. Mar Ecol Prog Ser 585:49–69

Gest N, Gautier H, Stevens R (2013) Ascorbate as seen through plant evolution: the rise of a successful molecule? J Exp Bot 64(1):33–53

Girolomoni L, Cazzaniga S, Pinnola A, Perozeni F, Ballottari M, Bassi R (2019) LHCSR3 is a nonphotochemical quencher of both photosystems in *Chlamydomonas reinhardtii*. Proc Natl Acad Sci 116:4212–4217

He Y, Fu J, Yu C, Wang X, Jiang Q, Hong J, Lu K, Xue G, Yan C, James A (2015) Increasing cyclic electron flow is related to Na+ sequestration into vacuoles for salt tolerance in soybean. J Exp Bot 66(21):6877–6889

Hertle AP, Blunder T, Wunder T, Pesaresi P, Pribil M, Armbruster U, Leister D (2013) PGRL1 is the elusive ferredoxin-plastoquinone reductase in photosynthetic cyclic electron flow. Mol Cell 49:511–523

Horton P, Park K-J, Obayashi T, Fujita N, Harada H, Adams-Collier C, Nakai K (2007) WoLF PSORT: protein localization predictor. Nucleic Acids Res 35(2):W585–W587

Hu W, Song X, Shi K, Xia X, Zhou Y, Yu J (2008) Changes in electron transport, superoxide dismutase and ascorbate peroxidase

isoenzymes in chloroplasts and mitochondria of cucumber leaves as influenced by chilling. Photosynthetica 46(4):581
Huang F, Chen K-S, Yip H-L, Hau SK, Acton O, Zhang Y, Luo J, Jen AK-Y (2009) Development of new conjugated polymers with donor− π-bridge− acceptor side chains for high performance solar cells. J Am Chem Soc 131(39):13886–13887
Huang W, Yang S-J, Zhang S-B, Zhang J-L, Cao K-F (2012) Cyclic electron flow plays an important role in photoprotection for the resurrection plant *Paraboea rufescens* under drought stress. Planta 235(4):819–828
Huang W, Yang Y-J, Hu H, Zhang S-B (2016) Seasonal variations in photosystem I compared with photosystem II of three alpine evergreen broad-leaf tree species. J Photochem Photobiol B 165:71–79
Huang W, Zhang S-B, Xu J-C, Liu T (2017) Plasticity in roles of cyclic electron flow around photosystem I at contrasting temperatures in the chilling-sensitive plant *Calotropis gigantea*. Environ Exp Bot 141:145–153
Hüner N, Dahal K, Hollis L, Bode R, Rosso D, Krol M, Ivanov AG (2012) Chloroplast redox imbalance governs phenotypic plasticity: the "grand design of photosynthesis" revisited. Front Plant Sci 3:255
Ivanov AG, Morgan RM, Gray GR, Velitchkova MY, Hüner NP (1998) Temperature/light dependent development of selective resistance to photoinhibition of photosystem I. FEBS Lett 430(3):288–292
Iwai M, Takizawa K, Tokutsu R, Okamuro A, Takahashi Y, Minagawa J (2010) Isolation of the elusive supercomplex that drives cyclic electron flow in photosynthesis. Nature 464(7292):1210–1213
Jeffrey SW, Humphrey GF (1975) New spectrophotometric equations for determining chlorophyll a, b, c1, c2 in higher plants, algae and natural phytoplankton. Biochem Physiol Pflanz 167:191–194
Julkowska M (2020) Extreme Engineering: How Antarctic Algae Adapt to Hypersalinity. Plant Physiol 183(2):427
Kalra I, Wang X, Cvetkovska M, Jeong J, McHargue W, Zhang R, Hüner N, Yuan JS, Morgan-Kiss R (2020) *Chlamydomonas* sp. UWO 241 Exhibits high cyclic electron flow and rewired metabolism under high salinity. Plant Physiol 183(2):588–601
Kovács L, Vidal-Meireles A, Nagy V, Tóth SZ (2016) Quantitative determination of ascorbate from the green alga *Chlamydomonas reinhardtii* by HPLC. Bio Protocols 6:2067
Kramer DM, Evans JR (2011) The importance of energy balance in improving photosynthetic efficiency. Plant Physiol 155:70–78
Kramer DM, Johnson G, Kiirats O, Edwards GE (2004) New fluorescence parameters for the determination of Q_a redox state and excitation energy fluxes. Photosynth Res 79(2):209–218
Kukuczka B, Magneschi L, Petroutsos D, Steinbeck J, Bald T, Powikrowska M, Fufezan C, Finazzi G, Hippler M (2014) Proton gradient regulation5-like1-mediated cyclic electron flow is crucial for acclimation to anoxia and complementary to nonphotochemical quenching in stress adaptation. Plant Physiol 165:1604–1617
Ledford HK, Chin BL, Niyogi KK (2007) Acclimation to singlet oxygen stress in *Chlamydomonas reinhardtii*. Eukaryot Cell. https://doi.org/10.1128/ec.00207-06LB-Ledford2007
Liefer JD, Garg A, Campbell DA, Irwin AJ, Finkel ZV (2018) Nitrogen starvation induces distinct photosynthetic responses and recovery dynamics in diatoms and Prasinophytes. PLoS ONE 13:1–24
Liu Y, Qi M, Li T (2012) Photosynthesis, photoinhibition, and antioxidant system in tomato leaves stressed by low night temperature and their subsequent recovery. Plant Sci 196:8–17
Lucker B, Kramer DM (2013) Regulation of cyclic electron flow in *Chlamydomonas reinhardtii* under fluctuating carbon availability. Photosynth Res 117(1–3):449–459
Maruta T, Ishikawa T (2017) Ascorbate peroxidases: crucial roles of antioxidant enzymes in plant stress responses. In: Hossain MA (ed) Ascorbic acid in plant growth, development and stress tolerance. Springer, Berlin, pp 111–127
Maruyama S, Tokutsu R, Minagawa J (2014) Transcriptional regulation of the stress-responsive light harvesting complex genes in *Chlamydomonas reinhardtii*. Plant Cell Physiol 55:1304–1310
Maxwell DP, Falk S, Trick CG, Huner NPA (1994) Growth a low temperature mimics high-light acclimation in *Chlorella vulgaris*. Plant Physiol 105:535–543
McNeill J, Barrie F, Buck W, Demoulin V, Greuter W, Hawksworth D, Herendeen P, Knapp S, Marhold K, Prado J (2012) International Code of Nomenclature for algae, fungi and plants. Regnum Vegetabile 154
Minagawa J (2011) State transitions—the molecular remodeling of photosynthetic supercomplexes that controls energy flow in the chloroplast. Biochim Et Biophys Acta-Bioenerg 1807(8):897–905
Møller IM, Jensen PE, Hansson A (2007) Oxidative modifications to cellular components in plants. Annu Rev Plant Biol 58:459–481
Morgan-Kiss R, Ivanov AG, Williams J, Mobashsher K, Hüner NP (2002a) Differential thermal effects on the energy distribution between photosystem II and photosystem I in thylakoid membranes of a psychrophilic and a mesophilic alga. Biochim Biophys Acta 1561(2):251–265
Morgan-Kiss RM, Ivanov AG, Hüner NPA (2002b) The Antarctic psychrophile, *Chlamydomonas subcaudata,* is deficient in state I-state II transitions. Planta 214(3):435–445
Morgan-Kiss RM, Ivanov AG, Modla S, Czymmek K, Hüner NP, Priscu JC, Lisle JT, Hanson TE (2008) Identity and physiology of a new psychrophilic eukaryotic green alga, *Chlorella* sp, strain BI, isolated from a transitory pond near Bratina Island, Antarctica. Extremophiles 12(5):701–711
Morgan-Kiss RM, Priscu JC, Pocock T, Gudynaite-Savitch L, Huner NP (2006) Adaptation and acclimation of photosynthetic microorganisms to permanently cold environments. Microbiol Mol Biol Rev 70(1):222–252
Morgan RM, Ivanov AG, Priscu JC, Maxwell DP, Hüner NPA (1998) Structure and composition of the photochemical apparatus of the Antarctic green alga, *Chlamydomonas subcaudata*. Photosyn Res 56:303–314
Mou S, Zhang X, Ye N, Dong M, Liang C, Liang Q, Miao J, Xu D, Zheng Z (2012) Cloning and expression analysis of two different LhcSR genes involved in stress adaptation in an Antarctic microalga *Chlamydomonas* Sp ICE-l. Extremophiles 16:193–203
Müller P, Li X-P, Niyogi KK (2001) Non-photochemical quenching. A response to excess light energy. Plant Physiol 125(4):1558–1566
Neale PJ, Priscu JC (1995) The photosynthetic apparatus of phytoplankton from a perennially ice-covered Antarctic lake: acclimation to an extreme shade environment. Plant Cell Physiol 36:253–263
Nichols HW, Bold HC (1965) *Trichosarcina polymorpha* Gen. Et Sp Nov J Phycol 1:34–38
Niyogi KK (1999) Photoprotection revisited: genetic and molecular approaches. Annu Rev Plant Biol 50(1):333–359
Noctor G, Foyer CH (1998) Ascorbate and glutathione: keeping active oxygen under control. Annu Rev Plant Biol 49(1):249–279
Öquist G, Huner NP (2003) Photosynthesis of overwintering evergreen plants. Annu Rev Plant Biol 54:329–355
Peers G, Truong TB, Ostendorf E, Busch A, Elrad D, Grossman AR, Hippler M, Niyogi KK (2009) An ancient light-harvesting protein is critical for the regulation of algal photosynthesis. Nature 462(7272):518–521
Pérez-Pérez ME, Couso I, Crespo JL (2012) Carotenoid deficiency triggers autophagy in the model green alga *Chlamydomonas reinhardtii*. Autophagy 8(3):376–388
Pitsch NT, Witsch B, Baier M (2010) Comparison of the chloroplast peroxidase system in the chlorophyte *Chlamydomonas reinhardtii*, the bryophyte *Physcomitrella patens*, the lycophyte

Selaginella moellendorffii and the seed plant *Arabidopsis thaliana*. BMC Plant Biol 10(1):133
Pocock T (2004) Phylogeny, photoinhibition and recovery of a new Antarctic psychrophile Chlamydomonas raudensis (UWO 241). Ph.D., University of Western Ontario, London
Pocock T, Koziak A, Rosso D, Falk S, Huner HPA (2007) *Chlamydomonas raudensis* ettl. (UWO241) exhibits the capacity for rapid D1 repair in response to chronic photoinhibition at low temperature. J Phycol 43:924–936
Pocock T, Vetterli A, Falk S (2011) Evidence for phenotypic plasticity in the Antarctic extremophile *Chlamydomonas raudensis* Ettl. UWO 241. J Exp Bot 62(3):1169–1177. https://doi.org/10.1093/jxb/erq347
Possmayer M, Gupta RK, Szyszka-Mroz B, Maxwell DP, Lachance MA, Hüner N, Smith DR (2016) Resolving the phylogenetic relationship between *Chlamydomonas* sp. UWO 241 and *Chlamydomonas raudensis* SAG 49.72 (Chlorophyceae) with nuclear and plastid DNA sequences. J Phycol 52(2):305–310
Raymond JA, Morgan-Kiss R (2013) Separate origins of ice-binding proteins in Antarctic *Chlamydomonas* species. PLoS ONE 8(3):e59186
Raymond JA, Morgan-Kiss R, Stahl-Rommel S (2020) Glycerol is an osmoprotectant in two antarctic *Chlamydomonas* species from an ice-covered saline lake and is synthesized by an unusual bidomain enzyme. Front Plant Sci 11:1259
Sharma P, Jha AB, Dubey RS, Pessarakli M (2012) Reactive oxygen species, oxidative damage, and antioxidative defense mechanism in plants under stressful conditions. J Bot 2012:217037
Sievers F, Higgins DG (2018) Clustal omega for making accurate alignments of many protein sequences. Protein Sci 27(1):135–145
Sirikhachornkit A, Niyogi KK (2010) Antioxidants and photo-oxidative stress responses in plants and algae. In: Govindjee X, Sharkey TD (eds) Advances in photosynthesis and respiration, vol 31. Springer, Dordrecht, pp 379–396
Smith BM, Morrissey PJ, Guenther JE, Nemson JA, Harrison MA, Allen JF, Melis A (1990) Response of the photosynthetic apparatus in *Dunaliella salina* (green algae) to irradiance stress. Plant Physiol 93(4):1433–1440
Strand DD, Livingston AK, Satoh-Cruz M, Froehlich JE, Kramer MVG (2015) Activation of cyclic electron flow by hydrogen peroxide in vivo. Proc Natl Acad Sci 112:5539–5544
Strzepek RF, Boyd PW, Sunda WG (2019) Photosynthetic adaptation to low iron, light, and temperature in Southern Ocean phytoplankton. Proc Natl Acad Sci USA 116:4388–4393
Suzuki N, Koussevitzky S, Mittler R, Miller G (2012) ROS and redox signalling in the response of plants to abiotic stress. Plant Cell Environ 35(2):259–270
Szyszka-Mroz B, Cvetkovska M, Ivanov AG, Smith DR, Possmayer M, Maxwell DP, Hüner NP (2019) Cold-adapted protein kinases and thylakoid remodeling impact energy distribution in an Antarctic psychrophile. Plant Physiol 180(3):1291–1309
Szyszka-Mroz B, Pittock P, Ivanov AG, Lajoie G, Hüner NP (2015) The Antarctic psychrophile, *Chlamydomonas* sp. UWO 241, preferentially phosphorylates a PSI-cytochrome b6/f supercomplex. Plant Physiol 169:717–736
Szyszka B, Ivanov AG, Hüner NP (2007) Psychrophily is associated with differential energy partitioning, photosystem stoichiometry and polypeptide phosphorylation in *Chlamydomonas raudensis*. Biochim Biophys Acta BBA (BBA) Bioenerg 1767(6):789–800
Takahashi S, Murata N (2008) How do environmental stresses accelerate photoinhibition? Trends Plant Sci 13(4):178–182
Takahashi H, Clowez S, Wollman FA, Vallon O, Rappaport F (2013) Cyclic electron flow is redox-controlled but independent of state transition. Nat Commun 4:1–8
Tanaka A, Melis A (1997) Irradiance-dependent changes in the size and composition of the chlorophyll *a-b* light-harvesting complex in the green alga *Dunaliella salina*. Plant Cell Physiol 38(1):17–24
Tardif M, Atteia A, Specht M, Cogne G, Rolland N, Brugière S, Hippler M, Ferro M, Bruley C, Peltier G (2012) PredAlgo: a new subcellular localization prediction tool dedicated to green algae. Mol Biol Evol 29(12):3625–3639
Teixeira FK, Menezes-Benavente L, Margis R, Margis-Pinheiro M (2004) Analysis of the molecular evolutionary history of the ascorbate peroxidase gene family: inferences from the rice genome. J Mol Evol 59(6):761–770
Van Alstyne KL, Sutton L, Gifford S-A (2020) Inducible versus constitutive antioxidant defenses in algae along an environmental stress gradient. Mar Ecol Prog Ser 640:107–115
Velitchkova M, Popova AV, Faik A, Gerganova M, Ivanov AG (2020) Low temperature and high light dependent dynamic photoprotective strategies in *Arabidopsis thaliana*. Physiol Plant 170:93–108
Venisse J-S, Gullner G, Brisset M-N (2001) Evidence for the involvement of an oxidative stress in the initiation of infection of pear by *Erwinia amylovora*. Plant Physiol 125(4):2164–2172
Wildi B, Lütz C (1996) Antioxidant composition of selected high alpine plant species from different altitudes. Plant Cell Environ 19(2):138–146
Wilson KE, Hüner NP (2000) The role of growth rate, redox-state of the plastoquinone pool and the trans-thylakoid DpH in photoacclimation of *Chlorella vulgaris* to growth irradiance and temperature. Planta 212(1):93–102
Witman GB (1993) *Chlamydomonas* phototaxis. Trends Cell Biol 3(11):403–408
Wu B, Wang B (2019) Comparative analysis of ascorbate peroxidases (APXs) from selected plants with a special focus on *Oryza sativa* employing public databases. PLoS ONE 14(12):10226543
Yamori W, Makino A, Shikanai T (2016) A physiological role of cyclic electron transport around photosystem I in sustaining photosynthesis under fluctuating light in rice. Sci Rep 6:20147
Young JN, Schmidt K (2020) Its whats inside that matters: physiological adaptations of high-latitude marine microalgae to environmental change. New Phytol 5:1307–1318
Zechmann B, Stumpe M, Mauch F (2011) Immunocytochemical determination of the subcellular distribution of ascorbate in plants. Planta 233(1):1–12
Zhang C, Liu J, Zhang Y, Cai X, Gong P, Zhang J, Wang T, Li H, Ye Z (2011) Overexpression of SlGMEs leads to ascorbate accumulation with enhanced oxidative stress, cold, and salt tolerance in tomato. Plant Cell Rep 30(3):389–398
Zhang S, Scheller HV (2004) Photoinhibition of photosystem I at chilling temperature and subsequent recovery in *Arabidopsis thaliana*. Plant Cell Physiol 45(11):1595–1602
Zhang X, Cvetkovska M, Morgan-Kiss R, Hüner NP, Smith DR (2021) Draft genome sequence of the Antarctic green alga *Chlamydomonas* sp. UWO241. Iscience 24(2):102084
Zheng Y, Xue C, Chen H, He C, Wang Q (2020) Low-temperature adaptation of the snow alga *Chlamydomonas nivalis* is associated with the photosynthetic system regulatory process. Front Microbiol 11:1233